Int. J. Heat Mass Transfer. Vol. 27, No. 11, pp. 2145–2154, 1984
Printed in Great Britain

0017-9310/84 $3.00 + 0.00
Pergamon Press Ltd.

Heat transfer from impinging jets to a flat plate with conical and ring protuberances

PETER HRYCAK

Mechanical Engineering Department, New Jersey Institute of Technology, Newark, NJ 07102, U.S.A.

(*Received* 22 *November* 1983 *and in revised form* 21 *March* 1984)

Abstract—An experimental investigation of heat transfer from round jets, impinging normally on a flat plate with exchangeable, heat transfer enhancing protuberances, has been carried out, and the pertinent literature surveyed, for Reynolds numbers ranging from 14 000 to 67 000, and nozzle diameters from 3.18 to 9.52 mm. The experimental data at the stagnation point indicated laminar flow, and a significant enhancement of heat transfer there, due to the introduction of the spike protuberance; the ring protuberance reduced the local heat flux somewhat. Data have also been correlated by means of dimensional analysis and compared with the conical flow theory.

INTRODUCTION

APPLICATIONS of round jets impinging on heated/cooled surfaces, held normal to the axis of flow, have been observed to produce relatively high heat fluxes. Thus, a substantial increase in heat transfer coefficients can be realized in this fashion, in comparison with the heat transfer rates obtainable by conventional methods of convective cooling or heating. Because of this vigorous local cooling/heating effect, impinging jets have attracted the attention of a large number of investigators. Among the investigators of jet heat transfer, the majority studied heat transfer between cold impinging jets and flat heated surfaces.

The earlier results on heat transfer from impinging jets have been summarized, for example, by Livingood and Hrycak [1], Martin [2], and Hrycak [3]. It appears that in spite of the existence of substantial theoretical foundations [4, 5], a theoretical explanation of the essential characteristics of heat transfer from impinging jets is not possible in all cases, and additional experimentation and analysis are indicated.

Therefore, the experimental approach and semi-empirical theory still are often used in the investigation of heat transfer from single, round, cold impinging jets. This is also the main topic of this paper. In particular, it is interesting to find out to what extent heat transfer from impinging jets may still be enhanced by addition of suitable protuberances to an originally flat target plate. Here, a cone protuberance in the center of the plate appears as very suitable. A ring protuberance at the external edge of the plate, which would enhance recirculation of air in the mixing cone of the original impinging jet, appeared as another logical choice. Also, a combined effect of both protuberances appeared worth a closer study. The experimental test setup is shown in Fig. 1.

Many aspects of impinging jet heat transfer can be best understood in terms of the related fluid flow data. In particular, flow over a cone has been investigated by Leuteritz and Mangler [6] and Evans [7] theoretically. This analysis applies also reasonably well to the effect of the cone protuberance in the center of a flat target plate on the local heat transfer. The region of the separated flow in the wall-jet area and the effect of ring protuberance cannot be treated analytically at present, and resort will have to be made to the dimensional analysis.

The comparison of the data of various investigators and analysis of new data are greatly simplified by the use of dimensional analysis. Thus, for the local value of the Nusselt number, Nu, one can expect, from the consideration of all the contributing variables for heat transfer from impinging jets, a relation involving Re_d, Pr, and $n+4$ characteristic linear dimensions

$$Nu = K\, Re_d^a\, Pr^b (Z_n/d)^c (d_{pl}/d)^d (x/d)^e \times (L_1/d)^f (L_2/d)^g \ldots (L_n/d)^n \quad (1)$$

where K, a, b, c, ..., etc., are ordinarily considered constants over the restricted ranges of the major independent variables, that can be evaluated either

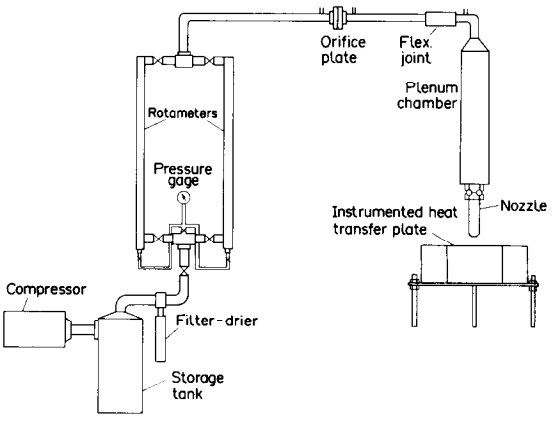

FIG. 1. Experimental test setup.

NOMENCLATURE

c_p specific heat at constant pressure [kJ kg^{-1} K^{-1}]
d nozzle diameter [mm]
d_{pl} plate diameter [mm]
$f(\eta)$ dimensionless stream function
F_p expression relating cone geometry to the given nozzle diameter
Fr Froessling number, $Nu/Re^{1/2}$
$g(\eta)$ dimensionless temperature function
h heat transfer coefficient [W m^{-2} K^{-1}]
k thermal conductivity [W m^{-1} K^{-1}]
K constant
K_p constant in equations (12a) and (13), K^*/F_p
L significant length [mm]
M distance from the surface of the flat plate to the bottom thermocouple [mm]
N distance between the top and bottom thermocouples [mm]
Nu_L Nusselt number, hL/k
Pr Prandtl number, $c_p\mu/k$
q exponent expressing Z_n/d dependence
Q heat flux [W]
Re_L Reynolds number, $u_{oc}L/\nu$
s height of lateral surface of the conical protuberance [mm]
T temperature [K]
u nozzle exit velocity, also velocity in the boundary layer parallel to the wall [m s^{-1}]
U free-stream velocity [m s^{-1}]
x distance away from the stagnation point, along cone generatrix, also along target plate [mm]
y distance away from target surface on the conical protuberance [mm]
Z_n distance from nozzle to the target plate [mm].

Greek symbols

β parameter related to free-stream pressure gradient
θ dimensionless temperature, $(T-T_w)/(T_\infty-T_w)$
μ dynamic viscosity [kg m^{-1} s^{-1}]
ν kinematic viscosity [m^2 s^{-1}].

Subscripts and other symbols

b bottom thermocouple
c center of symmetry
d, s, x dimensionless parameter with d, s, x as the significant length
eq Nusselt number based on h determined from equation (11a) with T_w replaced by $T_{w,eq}$, temperature of the protuberance at a reference section, flush with the flat plate surface
o origin; reference target-to-nozzle spacing
p index indicating target geometry and nozzle diameter, Tables 2 and 3
t top thermocouple
w conditions at surface of target
$\bar{}$ average (mean integral) value.

theoretically or experimentally. The terms L_1, L_2 may be specialized here as the characteristic dimensions of the protuberances used, for example.

The segmented plate used in the present experiments lent itself well to experiments where individual flat segments had to be replaced by segments with protuberances, as shown in Figs. 2 and 3.

Parameters investigated were air jets generated by nozzles of a diameter d = 3.18, 6.35 and 9.52 mm with the nozzle-to-plate spacing, Z_n/d, ranging from 5 to 20, with the nominal nozzle Reynolds number Re_d = 14000, 26000, 54000, and 67000, based on the air properties at the nozzle exit. The nozzles used were 108 mm long, and lip-equipped, with lip thickness, L, equal to d (Fig. 4) which were capable of producing a nearly flat velocity profile at the nozzle exit ($\bar{u} = 0.96u_{oc}$). They were insulated externally with tape to insure an adiabatic expansion. Air was supplied by a reciprocating compressor with a large settling tank, passing through a filter, rotameter, plenum chamber, and the nozzle. Individually calibrated thermocouples were used throughout for all heat transfer measurements.

THEORETICAL CONSIDERATIONS

Since the present target plate has a conical protuberance with an included angle $2\phi = 19°$ at the center, one can treat the heat transfer there as resulting from the flow over a cone. This kind of flow has already received a lot of attention [6, 7]. Best known is the case of supersonic flow over a cone, where the attached shock wave makes the surface pressure gradient zero [8]. With the help of Mangler's transformation, the resulting heat transfer is shown to be $\sqrt{3}$ times larger than that on a flat plate at zero angle of attack. For subsonic flow over a cone, where for the external flow the relation $U = Cx^n$ applies, the effect of the cone geometry and of the surface pressure gradients would have to be included for realistic results, however. The exponent n is related to the included cone angle 2ϕ as

$$n = 0.014445\phi + 0.428087\phi^2 - 0.064447\phi^3 \quad \text{for} \quad 0 < \phi < \pi/4 \tag{2}$$

based on calculations in ref. [7]. Also, $u = Uf'(\eta)$, etc., where $f(\eta)$ satisfies the continuity equation and the

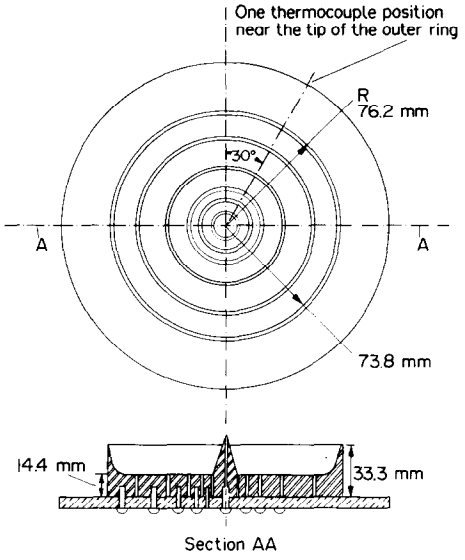

FIG. 2. Segmented plate with protuberances, top and side views.

momentum equation

$$f''' + ff'' + [2n/(3+n)](1-f'^2) = 0 \tag{3}$$

with $f(0) = f'(0) = 0$, and $f'(\infty) = 1$. The reduced coordinate η is here

$$\eta = (y/x)[(3+n)Ux/2v]^{1/2}. \tag{4}$$

On letting $2n/(3+n) = \beta$, equation (3) becomes identical with the Falkner–Skan equation. In terms of β, $n = 3\beta/(2-\beta)$; $\pi\beta$ is the included angle in the two-dimensional (2-D) potential flow over a wedge, with $U = Cx^{\beta/(2-\beta)}$. Here, β reflects the effect of the free-stream pressure gradient.

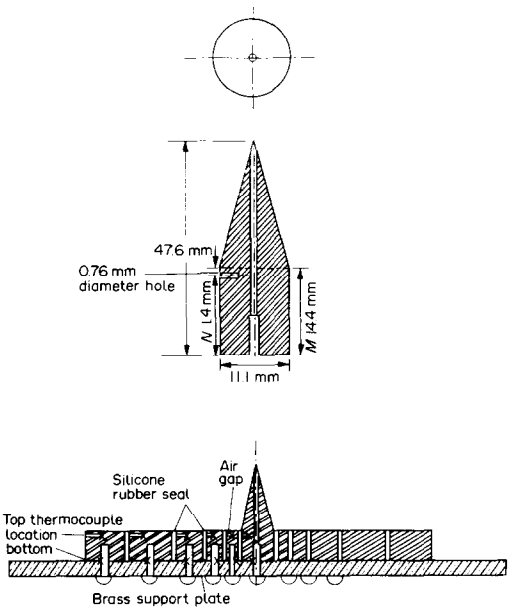

FIG. 3. Side view of plate with spike protuberance.

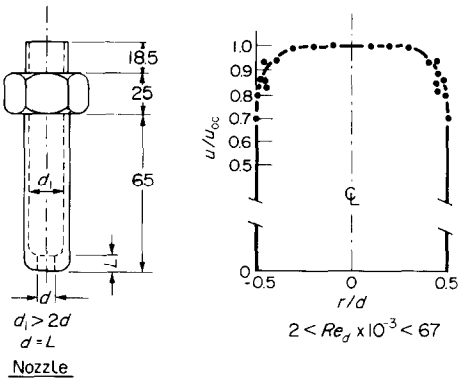

FIG. 4. Lip-equipped nozzle detail; velocity profile at nozzle exit.

The reduced coordinate η in equation (4) may also be expressed in terms of β

$$\eta = (y/x)\sqrt{3}[(Ux/v)/(2-\beta)]^{1/2}. \tag{5}$$

It has a 2-D counterpart

$$\bar{\eta} = (y/x)[(Ux/v)/(2-\beta)]^{1/2}. \tag{6}$$

It is seen that $\bar{\eta} = \eta/\sqrt{3}$.

The corresponding energy equation is, for constant wall temperature and low-speed flow

$$g'' + Pr\, fg' = 0 \tag{7}$$

with $\theta = g(\eta)$; $\theta(0) = 0$, $\theta(\infty) = 1$ if $\theta = (T - T_w)/(T_\infty - T_w)$. Since $q_w = h(T_w - T_\infty)$, and $h(T_w - T_\infty) = -k(\partial T/\partial y)_w$, the Nusselt number becomes here $Nu_x = (hx/k) = (g')_w \cdot \partial\eta/\partial y$, and there results, in the physical coordinates

$$Nu_x = (g')_w\sqrt{3} \cdot Re_x^{1/2}(2-\beta)^{-1/2} \tag{8}$$

on using η from equation (5) in the case of flow over a cone, while the use of equation (6) should be reserved for the 2-D flow. Equation (8) shows that a mere change from the properly formulated, reduced coordinates to the physical coordinates, produced here results directly applicable to the axisymmetric flow over a cone, that can be evaluated with the help of the already available expressions for g'_w from 2-D Falkner–Skan flow [7].

A polynomial approximation for g'_w for $Pr = 1$ and $0 \leqslant \beta \leqslant 0.5$ is

$$g'_w = 0.469600 + 0.217945\beta - 0.158373\beta^2. \tag{9}$$

Below are given examples on two well-known results. Thus, for $Pr = 1$, and letting $Fr_x = Nu_x/Re_x^{1/2}$, one obtains for $\beta = 0$: $Fr_x = \sqrt{3}(0.332057)$; for $\beta = 0.5$, $g'_w = 0.538979$, and $Fr_x = 0.762232$, which result is probably more accurate than the well-known Sibulkin's formula for axisymmetric stagnation flow [4]. Using Evans' data, for $0 \leqslant \beta \leqslant 0.5$ and $0.7 \leqslant Pr \leqslant 1.3$, the Prandtl number dependence of g'_w may be expressed by multiplication of g'_w for $Pr = 1$ with a factor $Pr^{0.35}$, with less than 1% error on the average. At $\beta = 0$, $Pr^{1/3}$ may be used, while at $\beta = 0.5$,

$Pr^{0.38}$ produces better results, when used together with equation (8).

In the problem at hand, $n = 0.0139$ according to equation (2), $\beta = 0.00922$, and $Fr_x = \sqrt{3}(0.332825)$, so that Fr_x is here only slightly higher than for the corresponding supersonic cone flow. Thus, for a cone with 19° included angle, the heat transfer for low-speed flow will be still virtually identical to that on a flat plate times $\sqrt{3}$. Also, the expression for average heat transfer for a cone with a lateral surface height s will be, for air with $Pr = 0.72$

$$\overline{Nu}_s = (4/\sqrt{3}) \cdot 0.333 Pr^{1/3} Re_s^{1/2} = 0.689 Re_s^{1/2} \quad (10)$$

where s is 33.7 mm long here. In the present experiment, $Re_s = Re_d(s/d)$, ranging from 5×10^4 to 7×10^5, seemed to assure the laminar flow regime on the cone protuberance.

EXPERIMENTAL TEST SETUP

The experimental apparatus, whose general layout is shown in Fig. 1, was made up of a basic flat target plate of 152.4 mm diameter, heated from below by condensing steam at atmospheric pressure, generated in a boiler with an electric immersion heater. The plate itself, made of Invar, consisted of five concentric segments with a 11.1 mm diameter center cylinder, and was 14.4 mm deep. In the target plate, the center cylinder and the outer segment could be replaced selectively by either of the protuberances shown in Figs. 2 and 3. Results obtained with the (flat) plate are shown elsewhere [9], while the effect of protuberances on local heat transfer on the segmented Invar plate is shown in Figs. 5–8. In the plate shown, the individual segments, separated from each other by a 1.6 mm air gap, sealed on top by a thin layer of silicone rubber, and equipped with thermocouples located 1.4 mm below the surface and at the base of each segment in the brass support plate, acted as calorimeters. Each segment had one bottom thermocouple; while the center segment had only one top thermocouple, segments 1 and 2 each had

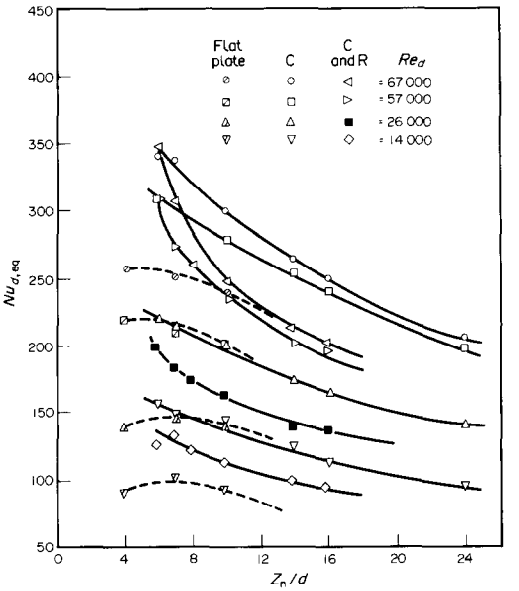

FIG. 6. Stagnation point results with cone and ring protuberances used, as function of nozzle-to-plate spacing, Z_n/d, and comparison with flat plate results; $d = 6.35$ mm.

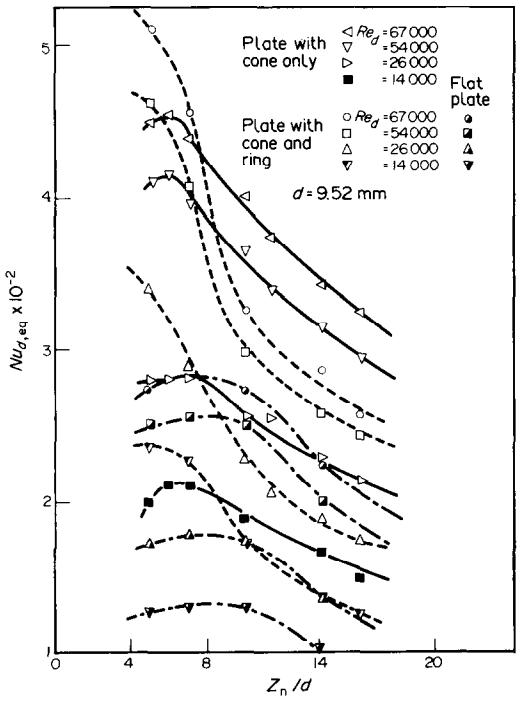

FIG. 5. Stagnation point results with cone and ring protuberances used, as function of nozzle-to-plate spacing, Z_n/d, and comparison with flat plate results; $d = 9.52$ mm.

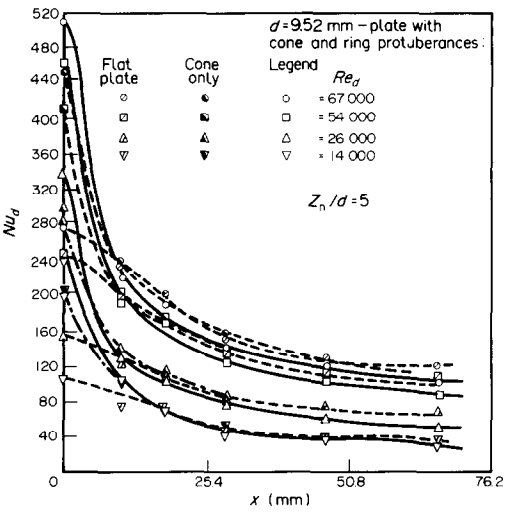

FIG. 7. Local distribution of heat transfer coefficients over a plate with protuberances and comparison with flat plate results; Nusselt numbers for plate with cone only, based on temperatures shown in Table 1, with $M/N = 1.108$, calculated according to equation (11b).

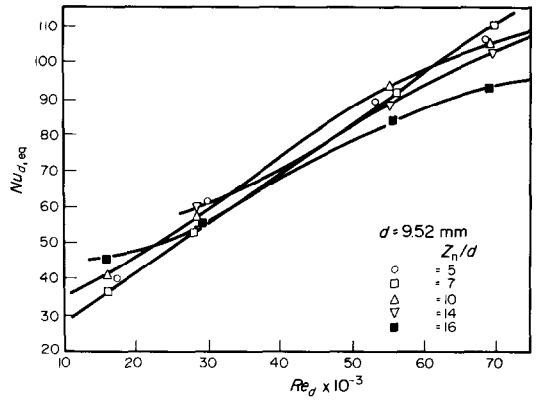

FIG. 8. Local effect of the ring protuberance on heat transfer on the outer segment.

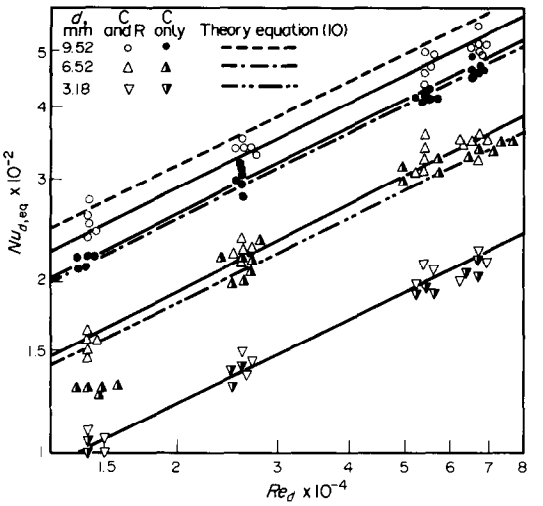

FIG. 9. Analysis of stagnation point results for all three nozzle diameters, plotted as a function of Re_d. Effects of plate geometry and nozzle diameter on local heat transfer. Comparison with theory (equation (10)).

two top thermocouples, and segments 3–5 had three top thermocouples each, arranged symmetrically around the circle forming the mean radius of a particular segment.

Thermal conductivity of the Invar used in fabricating the plate was tested separately [10], and given as $k_I = 13.6+0.019(T-273.15)$ W m^{-1} K^{-1} $\pm 3\%$. The cone and ring protuberances were made from AISI 302 stainless steel, with $k_{302SS} = 11.93+0.168(T-300)$ W m^{-1} K^{-1}, taken from the literature. In testing the overall heat balance, a flat plate, geometrically similar to the one shown in Fig. 3, was also used for the purposes of comparison. This plate was fabricated from AISI 304 stainless steel. It was used to test experimentally the overall effectiveness of the protuberances in modifying heat transfer from impinging jets on a flat plate. The particular metals listed here were chosen for their relatively high resistance to oxidation and their ability to keep the original surface finish. Also, it is believed that they represent reasonably well the behavior of alloys used in typical applications of jet cooling. A few additional details of the present experimental test set-up may be found in ref. [9].

EXPERIMENTAL RESULTS

The heat transfer coefficients were calculated from the relation

$$h = \left(\frac{k_{pl}}{N}\right)(T_b - T_t)/(T_w - T_{air}),$$

$$T_w = T_b + (T_t - T_b)(M/N) \quad (11a)$$

that can be transformed for the one-step Nusselt number determination into

$$Nu_d = [(d\bar{k}_{pl})/(\bar{k}_{air}N)]/[(T_b - T_{air})/(T_b - \bar{T}_t) - M/N] \quad (11b)$$

where $\bar{k}_{pl}$ was evaluated at $\bar{T} = \frac{1}{2}(T_b - \bar{T}_t)$, and $\bar{k}_{air}$ at $\bar{T} = \frac{1}{2}(T_{air} + \bar{T}_w)$. Here, subscript b refers to the bottom thermocouple, t to the top thermocouple, with N the distance between T_t and T_b, and M that between T_w and T_b, respectively. $\bar{T}_t$ represents the average temperature for the given segment's T_t readings. Equation (11a) is based on the notion of heat conductance of a typical calorimeter as that of a solid prism of metal. Contact resistance at all points of contact was reduced by application of a layer of silver powder filled high-conductivity grease.

In the present tests, the 11.1 mm diameter center segment had a 33.2 mm tall cone protuberance (Fig. 3), and the outer segment of the heat transfer plate was kept either flat or provided with an 18.8 mm ring protuberance (Fig. 2), to test their effect on the local and average heat transfer. The stagnation point results are shown in Figs. 5 and 6, as a function of the dimensionless target-to-plate spacings, Z_n/d. With the cone protuberance only, nearly a 60% heat transfer increase took place, while with both protuberances, that increase amounted to nearly 80% at its maximum, at the stagnation point for $Re_d = 54\,000$, for $d = 9.52$ mm, in comparison with flat plate results. The corresponding local heat transfer shows a substantial decline away from the stagnation point, however, as seen from Fig. 7, where data for $d = 9.52$ mm are shown for comparison. The local effect of the ring protuberance is shown in Figs. 8 and 10. In Figs. 5–7,* data applicable for a flat plate are also shown.

It is of interest to note that, when heat transfer-enhancing protuberances were used, the local heat transfer coefficient at the center of target plate was found to be very closely proportional to $Re_d^{1/2}$; this fact indicates a typical laminar boundary-layer flow over the cone protuberance. The correlation, for cone

* Some additional details of data that appear in Fig. 7 can be seen in Table 1.

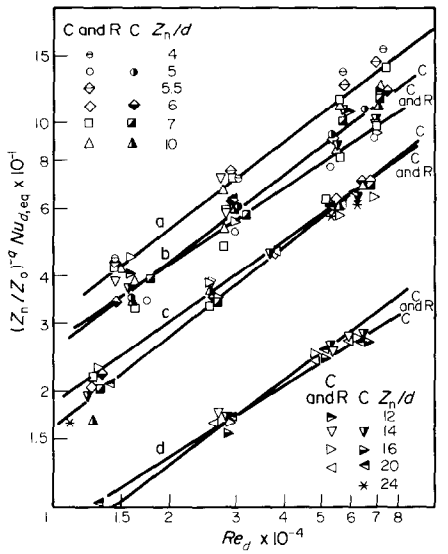

FIG. 10. Analysis of heat transfer results for the outer segment with the ring protuberance. Comparison with the corresponding flat plate result: (a) flat plate; (b) $d = 9.52$ mm; (c) $d = 6.35$ mm; (d) $d = 3.18$ mm.

protuberance only, was found to be, for the data shown in Figs. 5 and 6, of the form

$$Nu_{d,eq} = K_p\, Re_d^{1/2}(Z_n/Z_o)^q. \qquad (12a)$$

$Nu_{d,eq}$ is based on the nozzle diameter and the heat transfer coefficient that would have been measured in the case of an equivalent flat cylindrical center segment without the protuberance, as calculated by equation (11a). Equation (12a) is plotted in Fig. 9 and tabulated in Table 2. The index p is associated with the diameter of the nozzle used and the geometry of the protuberances. Thus, for $d = 6.35$ and 3.18 mm, the effect of recirculation provided by the ring is negligible, as $K_3 = K_4$ and $K_5 = K_6$. Z_o/d is the reference target-to-plate distance used for the particular nozzle diameter and the target geometry; $(Z_n/Z_o)^q$ reduces data taken at various Z_n values to a reference target-to-plate distance Z_o, for the sake of a better comparison. It is seen that q gets smaller as recirculation is decreased (as one changes from the cone and ring protuberance geometry to one with cone protuberance only) and as the nozzle diameter size is reduced.

To compare the present experimental results with the theoretical expression [equation (10)] they had to be converted from being based on d to s (the length of the side of the cone used) as the significant length, and expressed as an average over the side surface of the cone. This is accomplished by multiplying K_p in equation (12a) by the factor $F_p = d_{cone}/(2d_p^{1/2}s^{1/2})$. Then, letting $F_pK_p = K_p^*$, this results in the final expression to be used for comparison in Table 2

$$\overline{Nu}_s^* = K_p^*\, Re_s^{1/2}(Z_n/Z_o)^q. \qquad (12b)$$

The magnitude of $Re_s < 7 \times 10^5$, indicates still laminar flow here; division of the expression $\overline{Nu}_s^*(Z_n/Z_o)^{-q}$ from equation (12b) by equation (10) shows then to what degree the present results deviate from the theoretical laminar heat transfer in air over a cone. As could be expected, the deviation increases from 8% for $d = 9.52$ mm and the cone and ring geometry, to 34% for $d = 3.18$ mm, due to a decrease in flow velocity at the base of the cone and the inevitable flow separation there. Otherwise, the agreement between the theory (where heat transfer was based on constant wall temperature of the cone) and the experimental data is remarkably good. The present experimental results on heat transfer on the conical protuberance may be extrapolated even to a zero deviation between the thory and experiment, for a jet nozzle diameter being larger than, or equal to the cone diameter ($d_{cone} \leqslant d$). The calculations, supported by the appropriate measurements, indicate clearly that a conical protuberance at the center of a flat target plate definitively increases the heat flux there. In general, the heat transfer data for the 9.52 mm diameter nozzle show a similar agreement with the theory as the in-flight rocket data discussed by Knuth in ref. [11],* for example. The results in Table 2

* Compare also discussion of similar results on p. 271 of ref. [8].

Table 1. Temperature distribution in plate with cone protuberance

$Re_d \times 10^{-4}$	1.4		2.6		5.4		6.7	
T_{air}	301.5		301.4		299.0		299.1	
Segment No.	T_t*	T_b	T_t	T_b	T_t	T_b	T_t	T_b
0	344.5	375.3	338.5	368.5	332.8	368.0	331.3	371.4
1	356.2	369.4	350.5	368.0	344.9	367.2	342.8	370.4
2	360.8	370.5	354.8	369.4	348.5	368.5	346.4	369.7
3	363.3	371.2	358.4	370.4	352.1	369.4	350.3	368.6
4	366.0	371.8	360.9	371.4	355.5	370.3	353.6	366.8
5	367.8	372.3	365.1	371.8	361.4	371.3	359.8	367.7

* Note: T_t is the average of two readings, for segments 1 and 2, and it is the average of three readings, for segments 3–5, symmetrically spaced over each segment. All temperatures, taken with copper–constantan thermocouples in millivolts, have been converted to Kelvin.

Table 2. Effect of protuberances on heat transfer

d_p (mm)	p	K_p	F_p	K_p^*	Z_o/d	q_1 $\bar{q}_1 = 0.428$	Comparison with theory, equation (10), (%)	Geometry (C = cone, R = ring)
9.52	1	2.05	0.310	0.636	5	0.6	92.3	C & R
9.52	2	1.84	0.310	0.570	6	0.34	82.8	C only
6.35	3	1.35	0.380	0.513	6	0.56	74.5	C & R
6.35	4	1.35	0.380	0.513	6	0.31	74.5	C only
3.18	5	0.85	0.536	0.456	6	0.53	66.1	C & R
3.18	6	0.85	0.536	0.456	6	0.23	66.1	C only

and Fig. 9 show the effect of recirculation on enhancement of local impinging jet heat transfer: as the ring protuberance directs air flow away from the target plate, the flow patterns of the air entrained by the jet become affected, with the resulting enhancement of stagnation point heat transfer with respect to the average heat flux.

The local heat transfer at the outer segment is tabulated in Table 3, and is also shown in Figs. 8 and 10. It is an average of three readings taken at locations 120° apart, which is represented by an equation very similar to equation (12a)

$$Nu_{d,eq} = K_p Re_d^r (Z_n/Z_o)^q \qquad (13)$$

obtained by the least squares method, with a correlation better than 98%.

The equation constant K_p decreases with the nozzle diameter used. The power of the Reynolds number, r, is larger for a plate equipped with a cone at the center than for the plate with both cone and ring protuberances, except for the 3.18 mm diameter nozzle. The average value of r here is 0.719, quite close to the experimentally obtained power of the Reynolds number for the average heat transfer on the entire plate in question (without protuberances), 0.7 [9]. The Z_n/d dependence is also much less pronounced than at the center of plate ($\bar{q}_2 < \bar{q}_1$). The experimental values in Fig. 10 do not show any definitive trends for the Z_n/d dependence, but the observed powers of the nozzle Reynolds number indicate already turbulent flow, typical for a wall jet [1, 2]. From Fig. 8, the experimental heat transfer data in the wall jet region appear to be only marginally dependent on the target-to-plate spacing for $Z_n/d < 7$ also in the presence of a sharp discontinuity, and may be represented by a single formula, for all three diameters tested

$$Nu_d = 0.902 Re_d^{0.719}\, Pr^{1/3} (d/d_{pl})^{1.05}. \qquad (14)$$

Equation (14) shows the effect of the nozzle diameter, d, on heat transfer on the outer segment of the target plate of diameter d_{pl}, if d is varied and d_{pl} stays constant. Also, except for a small difference in the numerical constant (0.902 vs 1.32) and the power of Re_d, equation (14) is identical with the expression for the average Nusselt number for a flat plate, for the same range of Re_d and $Z_n/d < 7$ [9]. On the other hand, the flat plate results shown in Fig. 10 and summarized in Table 3 show that, in the absence of the ring protuberance, the outer segment heat transfer could be up to 35% higher, within the limits of the experimental error, estimated here with the help of equation (12b) as less than ±8%. As an example of the present heat transfer calculations, the temperatures used in calculating the local heat transfer distribution, for the plate with the conical protuberance only, are shown in Table 1, with the corresponding Nusselt numbers plotted in Fig. 7.

DISCUSSION OF EXPERIMENTAL RESULTS

There exist few experimental data on laminar heat transfer over a cone (protuberance) at moderate velocities, as most published results have been obtained at high Mach number speeds (cf. for example, Bogdonoff and Vas [12] and Knuth [11]). For many

Table 3. Outer segment heat transfer

d_p Nozzle diameter (mm)	p	K_p	Exponent of Re_d, r	Z_o/d	q_2 $\bar{q}_2 = 0.116$	Geometry (C = cone, R = ring)
9.52	1	0.0630	0.658	16	−0.132	C & R
9.52	2	0.0307	0.724	14	0.108	C only
6.35	3	0.0305	0.695	16	0.116	C & R
6.35	4	0.0129	0.776	20	0.164	C only
3.18	5	0.00668	0.760	20	0.375	C & R
3.18	6	0.0141	0.687	—	0	C only
9.52	7	0.0367	0.735	14	0.182	Flat plate

heat transfer applications, lower air speeds are desirable. The present experiments, with $Re_s < 7 \times 10^5$, show that heat transfer from jets impinging upon a conical protuberance follows reasonably well the trends to be expected from the laminar heat flow theory for flow over a cone, as shown in Fig. 9 and summarized in Table 2. In comparison, outer segment heat transfer data in Fig. 10 and in Table 3, show a decreased dependence of heat flux on the nozzle-to-plate spacing, as well as an increase in the applicable power of the Reynolds number in the resulting wall jet, trends that are similar to what could be also expected with jets impinging normally on a flat plate. There is a very noticeable increase in the heat flux at the spike protuberance, however. While the present experiments shed some light on the experimental verification on the theory of heat flow over a cone, they also show a practical way on how to increase the local heat transfer from impinging jets.

Thus, heat transfer enhancers in the form of spike and ring protuberances may substantially increase the local transfer intensity, but at some expense to the local heat transfer elsewhere, depending on the range of the nozzle Reynolds numbers investigated. The total heat transfer may not benefit at all from the presence of local heat transfer enhancers and changes in the geometry of the target plate. An overall heat balance for a plate with and without protuberances has been made, with some of these results shown in Table 4, but the results are inconclusive. The net effect of protuberances, incorporated into the segmented plate, has been a shift in local distribution of heat transfer intensity, but an overall heat transfer increase may have been prevented by formation of air pockets, due to the flow separation at the base of the ring protuberance. The elimination of 'pockets' due to flow separation would further increase impinging jet heat transfer on a plate with protuberances. Flow separation can also occur under certain circumstances at the base of the center spike protuberance. Fortunately, the extent of this separation must be moderate, as the effect of cone protuberances on heat transfer here could be analyzed successfully with the help of laminar boundary-layer theory of flow over a cone.

Mass transfer results have been very helpful in explanation of many impinging jet heat transfer phenomena [1, 2]. It appears, however, that for the more complex geometries, for example, like those involving the use of protuberances, together with high Reynolds numbers, direct heat transfer measurements are a practical necessity, for producing experimental heat fluxes close to their theoretical limit. It is believed that for nozzles that differed more significantly in geometry (e.g. those equipped with sharp-edged orifices) the results could have been different. It is important to remember that the nozzles used in the present experiments were of the lip-equipped tube type that had relatively good flow characteristics, with a flat velocity profile at the exit, and were likely to resemble the ones used in some representative applications. They produced at the stagnation point heat flux that peaked up at $Z_n/D \approx 7$ (cf. also refs. [1–3]). The effect of Prandtl number is discussed in the appendix. Although the present experiments were carried out with air only, comparisons have been made with the theoretical results that show a dependence on the Prandtl number. It appears that the use of a term like $Pr^{1/3}$ in equation (10) is justifiable. Otherwise, the slenderness of the present conical protuberance is the reason why equation (10) shows a heat flux only 0.2% higher than that on a cone in supersonic flow, which result, as outlined in refs. [8, 11], is also independent of the cone angle.

The present experimental results depend on two parameters, explicitly on the power q, an index related to the strength of the standing toroidal vortex generated by the conical outer ring, and implicitely on the fin effect of both protuberances. The vortex generated by recirculation is obviously due to the presence of the outer ring, that increases the recirculation, viewed as proportional to q, by 80, 80, and 130%, respectively, for each of the three nozzle diameters used. It leads also to a systematic and substantial increase in the average heat transfer over the cone in the center of the plate. This complex flow pattern is suggested, for example, by Sommerfeld's description of vortices associated with an ideal jet [13], and by the 'smoke wire' photographs of impinging real jets taken by Popiel and Trass [14]. The phenomenon of recirculation is a complex one and merits a separate investigation.

The fin effect of the protuberances used should be viewed as an enhancement of heat transfer when compared with a flat surface of the plate made of the same material, except when flow is separated. It is felt that the results obtained are more representative of the

Table 4. Comparison of heat losses through surface of plate (Q_1) with overall heat balance results (Q_2): nozzle diameter, 9.52 mm

Z_n/d	Re_d	Type of plate	Q_1 (W)	Q_2 (W)
4	67 000	Flat, made of 304 SS	304	327
7	54 000	Flat, made of 304 SS	245	229
4	67 000	With conical protuberance, Invar	286	285
7	54 000	With conical protuberance, Invar	254	257

Note: $Q_2 = Q_{\text{heater}} - Q_{\text{steam lost}} - Q_{\text{insulation}}$.

effects of impinging jets on heat transfer for the geometry at hand, than of the fins made of material with a given thermal conductivity. It is believed that the present experiments, the first ones of their kind, shall eventually lead to a more detailed investigation of the various phenomena described in the present paper.

An investigation of the fin effect of the conical protuberance was carried out. The resulting equation was very complicated, and it was decided, therefore, to postpone the detailed investigation of the conical fin protuberance effect on heat transfer from the impinging jets to some future time, to be included in a separate paper.

CONCLUSIONS

Experimental results for heat transfer between a flat plate with protuberances, and impinging, turbulent, cold air jets have been presented, for conditions applicable both inside and outside of the potential core. The results show a substantial increase in the stagnation point heat transfer, as well as some local heat transfer decrease under the ring protuberance.

For heat transfer at the spike protuberance, the experimentally obtained Nusselt number has been found to be reasonably close to an expression obtained through Mangler's transformation of the associated flat-plate flow problem. The average heat transfer for the entire target plate was found to be relatively little influenced by the protuberances used. The effects of the present heat transfer enhancers were demonstrated as conducive to a more vigorous spot cooling, however. Research still needs to be done on the basic mechanism of augmentation of heat fluxes resulting from impinging jets, for the most effective spot cooling.

Acknowledgements—This work has been partially supported by the National Science Foundation under the grant MEA-81-19471. It was also supported under the grant NGR-31-009-004. N. Shilling, D. Joseph, and J. Katzianer helped with collection and processing of the data.

REFERENCES

1. J. N. B. Livingood and P. Hrycak, Impingement heat transfer from turbulent air jets to flat plates—a literature survey, NASA TM X-2778 (1973).
2. H. Martin, Heat and mass transfer between impinging gas jets and solid surfaces, in *Advances in Heat Transfer* (edited by J. P. Hartnett and T. F. Irvine, Jr.), Vol. 13, pp. 1–60. Academic Press, New York (1977).
3. P. Hrycak, Heat transfer from impinging jets—a literature review, AFWAL-TR-81-3054, Flight Dynamics Laboratory, Wright-Patterson AFB, Ohio (1981).
4. M. Sibulkin, Heat transfer near the forward stagnation point at a body of revolution, *J. Aeronaut. Sci.* **19,** 570–571 (1952).
5. H. Schlichting, *Boundary-layer Theory* (7th edn.), p. 101. McGraw-Hill, New York (1979).
6. R. Leuteritz and W. Mangler, Die symmetrische Potentialströmung gegen einen Kreiskegel, *Unters. Mitt. Dtschr. Luftfahrtf.* **3226** (1945).
7. H. L. Evans, *Laminar Boundary-layer Theory*, pp. 95, 121. Addison-Wesley, Reading, Massachusetts (1968).
8. E. R. G. Eckert and R. M. Drake, Jr., *Heat and Mass Transfer*, p. 249. McGraw-Hill, New York (1959).
9. P. Hrycak, Heat transfer from round impinging jets to a flat plate, *Int. J. Heat Mass Transfer* **26,** 1857–1865 (1983).
10. D. R. Flynn, Calculation of thermal conductivity of an Invar sample from electrical resistivity data, NBS Report 9655 (1967). (Obtainable from the author.)
11. E. L. Knuth, Comments on "Flight measurements of aerodynamic heating and boundary-layer transition on the Viking 10 nose cone", *Jet Propul.* **26,** 1101–1103 (1956).
12. S. M. Bogdonoff and I. E. Vas, Preliminary investigation of spiked bodies at hypersonic speeds, *J. Aerospace Sci.* **26,** 65–74 (1959).
13. A. Sommerfeld, *Mechanics of Deformable Bodies, Lectures on Theoretical Physics*, Vol. 7, pp. 161–164. Academic Press, New York (1950).
14. C. O. Popiel and O. Trass, The effect of ordered structure of turbulence on momentum, heat and mass transfer of impinging round jets, *Proc. 7th Int. Heat Transfer Conf.*, Munich, Vol. 6, pp. 141–146 (1982).
15. H. Schrader, Trocknung feuchter Oberflächen mittels Warmluftstrahlen Strömungsvorgänge und Stöffübertragung, *VDI ForschHft.* 484 edn. B, **27,** 5–36 (1961).

APPENDIX

EFFECT OF PRANDTL NUMBER ON HEAT TRANSFER FROM JETS

The effect of Prandtl number on heat transfer from impinging jets is often expressed in the form Pr^m. Sibulkin's theoretical result [4] has $m = 0.4$; ref. [1] suggests $m = 0.36$–0.37. Schrader [15] obtained $m = 0.34$ from his own mass-transfer results (for the average of stagnation region and wall-jet results). He also mentions that Sherwood found $m = 1/3$ based on the survey of a large number of flat plate mass-transfer data. In this paper $m = 1/3$ is used for cases with a zero pressure gradient ($\beta = 0$), and $m = 0.38$ is suggested for $\beta = 0.5$, with $\bar{m} = 0.35$ for $0 < \beta < 0.5$, based on calculations of g'_w in ref. [7]. Therefore, for small β values, corresponding to flow over a slender cone, $m = 1/3$ appears to be appropriate, for Prandtl numbers in the range of 0.7–1.3.

TRANSFERT THERMIQUE POUR DES JETS FRAPPANT UNE PLAQUE PLANE AVEC DES PROTUBERANCES CONIQUES ET ANNULAIRES

Résumé—On conduit une recherche expérimentale sur le transfert thermique pour des jets ronds qui frappent normalement une plaque plane munie de protubérances augmentant le transfert thermique, pour des nombres de Reynolds allant de 14 000 à 67 000 et des diamètres d'orifice entre 3,18 et 9,52 mm. Les mesures au point d'arrêt indiquent un écoulement laminaire et un accroissement de transfert thermique dû à l'introduction de la protubérance pointue ; la protubérance annulaire réduit quelque peu le transfert de chaleur. Les données sont corrélées au moyen de l'analyse dimensionnelle et comparées avec la théorie de l'écoulement conique.

DER WÄRMEÜBERGANG VON PRALLSTRAHLEN AN EINE EBENE PLATTE MIT KONISCHEN UND RINGFÖRMIGEN ERHEBUNGEN

Zusammenfassung—Eine experimentelle Untersuchung des Wärmeüberganges von runden Strahlen, die senkrecht auf eine ebene Platte mit austauschbaren, den Wärmeübergang erhöhenden Erhebungen treffen, wurde für Reynoldszahlen zwischen 14000 und 67000 und Düsendurchmesser von 3.18 bis 9.52 mm durchgeführt und die dazugehörige Literatur gesichtet. Die experimentellen Daten am Staupunkt zeigten laminare Strömung an. Der Wärmeübergang am Staupunkt wurde durch die konischen Erhebungen wesentlich erhöht, während sich bei den ringförmigen Erhebungen eine geringfügige Erniedrigung des lokalen Wärmestromes einstellte. Die Daten wurden mit Hilfe der Dimensionsanalyse korreliert und mit der Theorie der konischen Strömung verglichen.

ТЕПЛОПЕРЕНОС ОТ УДАРЯЮЩИХСЯ СТРУЙ К ПЛОСКОЙ ПЛАСТИНЕ С ШЕРОХОВАТОСТЬЮ В ФОРМЕ КОНИЧЕСКИХ И КРУГЛЫХ ВЫСТУПОВ

Аннотация—Проведено экспериментальное исследование переноса тепла от круглых струй, падающих под прямым углом на плоскую пластину, на которой помещались сменные элементы шероховатости, интенсифицирующие теплоперенос. Дан обзор опубликованных данных для случаев, в которых число Рейнольдса изменялось в диапазоне от 14000 до 67000 и диаметров сопла от 3,18 до 9,52 мм. Экспериментальные данные, полученные в точке торможения, свидетельствуют о ламинарном характере течения и о значительной интенсификации теплопереноса при использовании выступов острой конической шероховатости; круглые выступы несколько снижали величину локального теплового потока. Полученные данные рассматривались также с помощью анализа размерностей и сравнивались с результатами, полученными из решения задачи обтекания конуса.